THE SHAPES OF FRAGMENTS FROM CATASTROPHIC DISRUPTION EVENTS: EFFECTS OF TARGET SHAPE AND IMPACT SPEED. A. Campo Bagatin[1,2,3], D. D. Durda[1], R. A. Alemañ[2,3], G. J. Flynn[4], M. M. Strait[5], A. N. Clayton[5], E. B. Patmore[5]. [1]Southwest Research Institute, 1050 Walnut Street, Suite 300, Boulder, CO 80302, USA, (acb@ua.es), [2]IUFACyT, Universidad de Alicante (Spain), [3]Dept. Física, ISTS, Universidad de Alicante (Spain), [4] Dept. of Physics, SUNY-Plattsburgh, NY (USA), [5] Department of Chemistry, Alma College, Alma, MI (USA).

Introduction: Recent experiments show 'onion shells' of fragments from impacts into spherical targets ([1], [2]). [3] suggest two modes of catastrophic disruption for spherical targets: (1) 'core-type' fragmentation in high-speed, high-energy-density regime; and (2) 'cone-type' fragmentation in low-speed, low-energy-density regime. Because of the propensity of previous laboratory investigations to focus on idealized spherical targets, there is a bit of ambiguity in decoupling the relative importance/influence of low speed or spherical shape in producing the 'onion shell' fragment shape outcomes. If due primarily to impact speed/energy density as suggested by [3], this could play an important role in main belt impacts due to the presence of non-spherical targets and non-negligible probability of low-speed (i.e., below about 3-4 km/s, subsonic in rock) impacts ([4]).

Impact Experiments: We used basalt samples obtained from a recent lava flow exposed in a road cut in Flagstaff, AZ. To examine explicitly the effects of target shape in determining impact outcome we chose to conduct impact experiments on both spherical and naturally-occurring irregularly-shaped targets of the same basalt material. These targets ranged in mass from 238 to 534 g. We measured the bulk density of each basalt sphere and several representative samples of the irregularly-shaped basalt targets. We obtained values of 2.95 (irregular) to 2.98 (spheres) g/cm^3 for the samples.

We impacted a total of six targets (two spheres and four irregular targets). The mean impact speed for asteroids in the main belt is ~5 km/sec ([4]), so we focused on shots with impact speeds in the ~4 to 6 km/s range. For each impact the projectile was a 3/16th inch diameter Al sphere fired at the specified using the NASA AVGR. The targets were each suspended at the center of the AVGR impact chamber from a thin nylon line.

Following each shot, the debris were collected from the floor of the AVGR chamber. This process typically recovered >95% of the target mass. Large fragments (>0.20 g) that were collected from the chamber were individually weighed, allowing us to carefully measure the mass-frequency distribution of the largest fragments from each impact experiment.

Figure 1. Our typical irregularly shaped and spherical targets.

High-speed video of each impact was obtained by five different video cameras (two Phantom V10s, one Phantom V12.1, and two Shimadzu HPV-1s), with frame rates ranging from 1,900 to 125,000 frames per second, to aid interpretation of the fragmentation mode of the targets.

The 36 largest fragments of each shot were photographed and their largest axes (a and b) accurately measured by the program "ImageJ". Their shortest axes (c) were measured by means of a digital caliber.

Figure 2. Typical shapes of the largest fragments resulting from hiper-velocity shattering impact experiments at AVGR.

In order to understand what is the bulk macroporosity of a non coherent set of fragments, we gathered randomly together the fragments with weighted

mass (58 to 90% of original targets masses) mimicking the post-shattering gravitational reaccumulation of fragments into an asteroid rubble-pile. For each set, we wrapped the fragments in a thin plastic film and measured the bulk volume inside the film shell by plunging it into distilled water while hanging it. The measured apparent weight is, in such conditions, the weight of the water displaced by the wrapped fragments. The volume is calculated straightforward from the density of water at the given temperature.

Results and Discussion: Cumulative mass distributions are derived and exponents $0.75<\beta<1.2$ are found for the relationship $N(>m)=Am^{-\beta}$ (m is the fragment mass, A is the corresponding constant) in the stationary part of the distribution. The exponent of each distribution and the mass of each largest fragment are found to be related to the corresponding specific energy of each impact as expected ([3]). The mass distributions seem to show slightly larger values of β in the case of spherical targets when comparing two sets of close specific energy impacts. However, this feature needs further sets of impact experiments to be properly investigated.

As for the shapes of fragments, b/a and c/a ratios were calculated along with the shape metrics $\Psi=(c2/ab)1/3$, $F=(a-b)/(a-c)$ for deviation from spherical shape and relative flatness respectively ([5] and [6]). The average relationship between a, b and c axes is 1:0.7:0.4, slightly different (flatter) than reported by former investigations (1:0.7:0.5) carried on in the 70s and 80s [7]. These result is quite stable and no differences are found in average shapes among spherical and irregular targets nor for different specific energy up to a factor of ~3. This does not mean that fragments look like 3-axial ellipsoidal shapes, instead they are quite irregular but their average relative sizes are distributed very nicely as described.

From a qualitative point of view, the high speed cameras at 1900 frames/s clearly show that shell-like fragments can be produced in shattering events *not* in the target's surface. Instead, shell-like fragments may form around the core fragment, well inside the target structure, independently on the target shape itself. This is a feature not reported to date.

Finally, the study of the macro-porosities of randomly aggregated fragments shows values in the 45 to 50% range. This result may be useful in the interpretation of small asteroids' bulk densities and in the calibration of numerical modelling of internal structures.

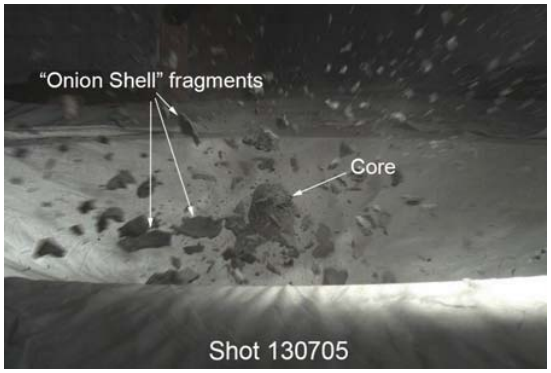

Figure 3. Frame showing the occurrence of circum-core fragments with shell shapes.

References: [1] Durda et al. (2011). Icarus, 211, 849-855. [2] Nakamura et al., 2013, CD8 workshop. [3] Fujiwara, A. et al. (1989) Asteroids II, UAP, 240-265. [4] Bottke W. F. et al. (1994), Icarus 107:255–268. [5] Benn, D. I., and C. K. Ballantyne (1993), Earth Surface Processes and Landforms, 18, 665–672. [6] Ehlmann, B. L et al. (2008), J. Geophys. Res., 113, F02012, doi:10.1029/2007JF000872. [7] Capaccioni et al. (1986), Icarus, 66, 487-514.